

Quasi-stationary tidal evolution with arbitrarily misaligned orbital and stellar angular momenta with a preliminary numerical investigation in the non-dissipative limit

Pavel Ivanov^{1,*} and John Papaloizou^{2,†}

¹*Astro Space Centre, P.N. Lebedev Physical Institute,
84/32 Profsoyuznaya Street, Moscow, 117997, Russia*

²*DAMTP, Centre for Mathematical Sciences,
University of Cambridge, Wilberforce Road, Cambridge CB3 0WA*

We review and extend the results of our 2021 paper concerning the problem of tidal evolution of a binary system with a rotating primary component with rotation axis arbitrarily inclined with respect to the orbital plane. Only the contribution of quasi-stationary tides is discussed. Unlike previous studies in this field we present evolution equations derived 'from first principles'. The governing equations contain two groups of terms.

The first group of terms determines the evolution of orbital parameters and inclination angles on a long time scale determined by the rate of energy dissipation often described as a 'viscous' time scale though radiative damping may also be included. It can be shown that these terms are formally equivalent to corresponding expressions obtained by other authors after a map between the variables adopted is established.

The second group of terms is due to stellar rotation. These terms are present even when dissipation in the star is neglected. They may lead to conservative evolution of the angles specifying the orientation of the stellar rotation axis and the orbital eccentricity vector on a relatively short time scale. The corresponding evolution is also linked to the rate of apsidal precession of the binary orbit. Unlike in our 2021 paper we consider all potentially important sources of apsidal precession in an isolated binary, namely precession arising from the tidal distortion and rotation of the primary as well as Einstein precession. We solve these equations numerically for a small sample of input parameters, leaving a complete analysis to an accompanying paper. Periodic changes to both the inclination of the rotational axis and

its precession rate are found. In particular, for a particular binary parameters periodic flips between prograde and retrograde rotation are possible. Also, when the inclination angle is allowed to vary, libration of the apsidal angle becomes possible. Furthermore, when the spin angular momentum is larger than the orbital angular momentum there is a possibility of a significant periodic eccentricity changes similar those coming about from the well-known Kozai-Lidov effect.

These phenomena could, in principle, be observed in systems with relatively large inclinations and eccentricities such as e.g. those containing a compact object. In such systems both large inclinations and eccentricities could be generated as a result of a kick applied to the compact object during a supernova explosion.

I. INTRODUCTION

Tidal interactions play an important role in many close binary systems including those containing a compact object, exoplanet systems, as well as our own Solar system (see e.g.[15] for a review). In this paper we begin by reviewing the main results obtained in our paper [10], hereafter IP, where we considered tidal interactions, in the regime of quasi-static tides, in a binary system consisting of a primary component with spin angular momentum that is arbitrarily misaligned with the angular momentum of the orbit. The companion is assumed to be compact and initially to have no internal degrees of freedom, though this was later relaxed to allow for energy dissipation in its interior that can contribute to the circularisation of the orbit.

This configuration setup is the same as that of Eggleton et. al. [5], hereafter EKH, who derived the force and couple on a binary orbit that arises from the dissipation associated with the equilibrium tide under the ad hoc assumption, that the rate of dissipation of energy is a positive definite function of the rate of change of the primary quadrupole tensor, viewed in a frame rotating with the star. Coriolis forces were neglected.

Contrary to EKH, in [10] we calculate the response of the primary to tidal forcing from

*pbi20@cam.ac.uk

†J.C.B.Papaloizou@damtp.cam.ac.uk

first principles in the low tidal forcing frequency limit, starting from the Navier-Stokes equations for a slightly perturbed gravitating and slowly rotating gas sphere. We adopt a quasi-static approximation, where in the leading approximation the stellar configuration is in hydrostatic equilibrium under the action of tidal forces. Motions associated with the equilibrium tide, dissipative processes and the effect of the Coriolis force are included as next order corrections, up to to first order in the primary rotational frequency, while neglecting the toroidal component of the response.

Our approach removes any need for ad hoc assumptions about these phenomena such as connecting them with the behaviour of the quadrupole tensor and provides a complete form for the response displacement without the need for assumptions about unknown functions made by Eggleton et. al. [5]. We use the next order corrections mentioned above to determine the effect of the tidal interaction on the orbit and angles characterising the orientation of the primary's rotational axis. These terms lead to precession of the primary rotation axis and orbital plane, which is added to that induced through orbital torques and stellar centrifugal distortion, in addition to non-dissipative evolution of the angle between the orbital and spin angular momenta referred hereafter to as 'inclination angle'.

It was shown by [10], that the rate of the evolution of the inclination angle is determined by apsidal precession rate. In [10] the simplest situation where the apsidal precession is due only to the presence of quasi-static tides, (see e.g. [20]) was considered. Here and in our accompanying paper [11] we consider a more general setting where the apsidal precession is determined by all processes expected for an isolated binary system. Namely, we consider relativistic Einstein precession, precession arising from tidal distortion induced by quasi-static tides and apsidal precession arising from rotation of the primary, see e.g. [2] and [19], [17] for a discussion of the latter term and its possible observational consequences. Since the apsidal precession rate determined by rotational effects depends on the inclination angle, equations governing the evolution of the inclination and the longitude of periastron are coupled. Under certain conditions this coupling could lead to non-trivial effects, e.g. libration of the apsidal line or a significant evolution of the inclination angle. Also, for systems with certain parameters, considerable evolution of the eccentricity results as a consequence of the conservation of total angular momentum of the system. In this paper we provide a preliminary numerical analysis of the corresponding evolution equations and identify certain potentially interesting regimes of evolution. In an accompanying paper [11] we provide an

extensive analytic treatment of this problem. This enables one to find out which effects, alone or in combination, are important for determining the apsidal precession rate, and the evolution of the angle of inclination between the orbital and spin angular momenta, for a given set of parameters of the system.

The plan of this paper is as follows. In Section II we give some basic definitions and define the three coordinate systems that are used to represent the dynamics of a binary with misaligned orbital and primary spin angular momenta. We introduce our set of equations for the determination of the orbital and spin angular momentum vectors in Section III. The form of the torque components acting on the star is then described in Section IV A. Expressions for the evolution of the semi-major axis and eccentricity are given in Section IV D. The potential contribution of non-dissipative terms arising through the effects of rotation, including the Coriolis force, to the orbital evolution are then discussed in Section V. In Section VII we review and discuss our results.

II. BASIC DEFINITIONS AND EQUATIONS

In this Section we describe the basic model setup and coordinate systems as used in IP.

A. Basic model

For simplicity, we consider a binary system for which one of the components acts as a point mass, i.e. it has no internal degrees of freedom referred to hereafter as the companion ¹. The other component, referred to hereafter as the primary possesses a distributed mass and a spin angular momentum which is unrestricted in orientation with respect to the orbital angular momentum. Thus, both these angular momenta are allowed to evolve with the resultant total angular momentum being conserved.

It is easy to show that the evolution of the angular momentum vectors is fully determined by four simple governing equations following from the law of conservation of angular momentum once the torques acting on the star are specified. Calculation of the energy exchange with the orbit and the law of conservation of energy then enables a complete description

¹ Note that IP also discuss the possibility of an extended companion of low mass, whose spin is fully synchronised to the orbit.

of the evolution of the system once a prescription to determine the evolution of the orbital apsidal line is prescribed. This is determined by the tidal interaction as well as the possible influence of other orbiting bodies. In the former case, to lowest order this is determined by the classical theory of apsidal motion as indicated in IP.

B. Coordinate system and notation

We introduce three reference frames. The first is a Cartesian coordinate system in a frame with origin at the centre of mass of the primary, and for which the direction of the conserved total angular momentum of the system, \mathbf{J} , defines the Z'' axis. The corresponding X'' and Y'' axes are located in the orthogonal plane.

The second one is a Cartesian frame such that the orbital angular momentum, \mathbf{L} , defines the direction of the Z' axis. This is inclined to the total angular momentum vector, \mathbf{J} , with an inclination i which need not be constant as the orbital angular momentum is not conserved.

The third (X, Y, Z) coordinate system, described as the stellar frame, is defined as in [9] with z -axis being directed along the direction of the stellar angular momentum vector, \mathbf{S} . The azimuthal angle associated with both \mathbf{J} and \mathbf{S} measured in the (X', Y', Z') system is $\pi/2 - \gamma$. The Y axis lies in the orbital plane and defines the line of nodes as viewed in the (X, Y) plane as in [9]. Note that the X', Y' and Y axes are coplanar as are the Z, Z' and Z'' axes. For a Keplerian orbit with fixed orientation, the line of apsides can be chosen to coincide with the X' axis. In this case the angle between this line and the X' axis, which we shall more generally denote by ϖ , will simply be given by $\varpi = 0$. Note that the angle between the apsidal line and the Y axis, being the line of nodes can be taken quite generally to be given by $\varpi + \gamma - \pi/2$ (with this choice it increases under positive rotation of the apsidal line in the orbit frame).

The coordinate systems are illustrated in Fig. 1.

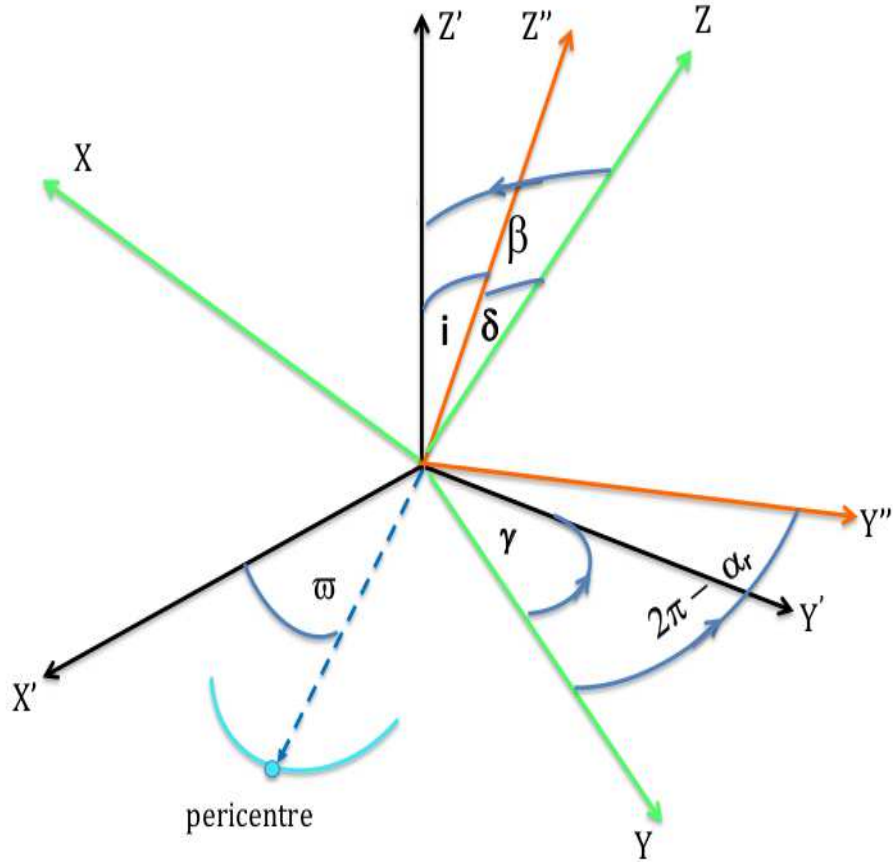


Figure 1: Illustration of the (X, Y, Z) and (X', Y', Z') coordinate systems together with the direction of the total angular momentum, which coincides with the Z'' axis of a coordinate system that is fixed in the primary centred frame. Note that the X', Y' and Y axes are coplanar as are the Z, Z' and Z'' axes. The angle between the angular momentum vectors \mathbf{L} , directed along the Z' axis and \mathbf{S} directed along the Z axis is β . The angle between \mathbf{L} and the Z'' axis directed along \mathbf{J} is i and $\delta = \beta - i$. The angle between the Y'' axis and the Y axis $2\pi - \alpha_r$. The apsidal line, the location of pericentre and an orbital arc in its neighbourhood are shown.

III. EVOLUTION EQUATIONS FOR THE ANGULAR MOMENTUM VECTORS

In this section we use the conservation of the total angular momentum to derive equations for the evolution of the magnitudes of the orbital and spin angular momenta L and S , and the angles β , $\delta = \beta - i$, and $\bar{\alpha} \equiv 2\pi - \alpha_r$, see Fig. 1 for the definition of these angles.

From the definition of β given above it follows that

$$\cos \beta = \frac{(\mathbf{L} \cdot \mathbf{S})}{LS}, \quad (1)$$

where L and S are the magnitudes of \mathbf{L} and \mathbf{S} , and

$$\cos i = \frac{(\mathbf{J} \cdot \mathbf{L})}{JL}, \quad (2)$$

where J is the magnitude of $\mathbf{J} = \mathbf{L} + \mathbf{S}$. We introduce the torque \mathbf{T} exerted on the star due to the tidal interaction. From the constancy of the total angular momentum $\mathbf{J} = \mathbf{L} + \mathbf{S}$ it follows that in the primary centred frame

$$\mathbf{T} = \dot{\mathbf{S}} = -\dot{\mathbf{L}}, \quad (3)$$

where a dot over a quantity, here and subsequently, indicates the time derivative of that quantity.

In addition, we also have $2\mathbf{J} \cdot \mathbf{L} = J^2 + L^2 - S^2$ and $2\mathbf{L} \cdot \mathbf{S} = J^2 - L^2 - S^2$. and, accordingly the cosines of β and i are given by,

$$\cos \beta = \frac{J^2 - L^2 - S^2}{2LS} \quad \text{and} \quad \cos i = \frac{J^2 + L^2 - S^2}{2JL}. \quad (4)$$

From these relations we can also express the sines of β , i and δ in terms of J , L and S , thus obtaining

$$\sin \beta = \frac{\sqrt{(J^2 - (L - S)^2)((L + S)^2 - J^2)}}{2LS}, \quad \text{and} \quad \sin i = \frac{\sqrt{(S^2 - (J - L)^2)((J + L)^2 - S^2)}}{2JL}. \quad (5)$$

In addition, consideration of the angular momentum components perpendicular to \mathbf{J} and \mathbf{S} respectively gives

$$\sin \delta = \frac{L}{S} \sin i = \frac{L}{J} \sin \beta. \quad (6)$$

We now make use of rotation matrices, which enable the transformation of the components of any vector from its representation in the stellar frame to its representation in the orbit

frame, and similarly its representation in the stellar frame to its representation in the primary centred frame. From these transformations and their inverses (see IP for further discussion) it is straightforward to express the components of \mathbf{L} , \mathbf{S} and the torque $\mathbf{T} = -\dot{\mathbf{L}}$ in the primary centred frame in terms of L , S and the components of the torque in the stellar frame ².

In this way the components of \mathbf{L} in the primary centred frame, $(L^{x''}, L^{y''}, L^{z''})$, are found to be given by

$$L^{x''} = L \cos \bar{\alpha} \sin i, \quad L^{y''} = -L \sin \bar{\alpha} \sin i \quad \text{and} \quad L^{z''} = L \cos i. \quad (7)$$

Similarly, the components of \mathbf{S} in the same frame, $(S^{x''}, S^{y''}, S^{z''})$, are given by

$$S^{x''} = -S \cos \bar{\alpha} \sin \delta, \quad S^{y''} = S \sin \bar{\alpha} \sin \delta, \quad \text{and} \quad S^{z''} = S \cos \delta, \quad (8)$$

and the components of \mathbf{T} in this frame, $(T^{x''}, T^{y''}, T^{z''})$, are given by

$$T^{x''} = \sin \bar{\alpha} T^y + \cos \bar{\alpha} T^1, \quad T^{y''} = \cos \bar{\alpha} T^y - \sin \bar{\alpha} T^1, \quad \text{and} \quad T^{z''} = \sin \delta T^x + \cos \delta T^z, \quad (9)$$

where $T^1 = \cos \delta T^x - \sin \delta T^z$ (10)

with the components of \mathbf{T} in the stellar frame being given by (T^x, T^y, T^z) .

From equation (3) together with equations (6) - (10) it is easy to obtain the following set of equations

$$\frac{di}{dt} = \frac{1}{L}(-\cos \beta T^x + \sin \beta T^z), \quad \frac{dL}{dt} = -\cos \beta T^z - \sin \beta T^x, \quad \frac{d}{dt} \bar{\alpha} = \frac{T^y}{\sin i L} = \frac{J}{LS} \frac{T^y}{\sin \beta}, \quad (11)$$

and

$$\frac{d}{dt} \delta = -\frac{T^x}{S}, \quad \dot{S} = T^z. \quad (12)$$

Note that we use (6) to obtain the last equality in (11). Also note that it is easy to check that $J^i = L^i + S^i$ are indeed first integrals of the set of equations (11) and (12).

Using the first equation of (11) together with (12) it is straightforward to obtain the evolution equation for angle β :

$$\frac{d\beta}{dt} = -\left(\frac{\cos \beta}{L} + \frac{1}{S}\right) T^x + \frac{\sin \beta}{L} T^z. \quad (13)$$

² We recall that by definition the components of \mathbf{L} in the orbit frame are $(0, 0, L)$ and the components of \mathbf{S} in the stellar frame are $(0, 0, S)$

Together with the energy conservation law equations (11) and (12) form a complete set for our model once the torque components are specified.

Note that an evolution equation for the angle γ is absent. This is because, physically, only the angle $\bar{\alpha} = 2\pi - \alpha_r$ appears in the specification of the orientation of the angular momentum vectors in the primary centred frame. In addition, only the angle between the apsidal line and the projection of the stellar spin angular momentum vector onto the orbital plane, $\varpi + \gamma$ matters for the determination of the orbital evolution. The evolution of this angle should be found from other considerations which are not based on the law of angular momentum conservation. This evolution is determined, in general, from tidal interactions, stellar flattening, General Relativity and/or a presence of other perturbing bodies, see below.

IV. THE RATE OF CHANGE OF THE ORBITAL ELEMENTS

In order to specify how the orbital elements change we begin by providing expressions for the torque components acting in the stellar frame.

A. Expressions for the components of the torque acting on the star

The torque components in the stellar frame to be used in equations (11) - (13) were derived in IP. The explicit expressions for them are as follows:

$$T^z = T_* (2\delta_1 \cos \beta \phi_1 - \delta_2 (1 - e^2)^{3/2} ((1 + \cos^2 \beta) \phi_2 - \sin^2 \beta \cos 2\hat{\omega} \phi_3)) \quad \text{and} \quad (14)$$

$$T \equiv T^x - iT^y =$$

$$T_* \sin \beta ((2\delta_1 - i\delta_3) \phi_1 - (1 - e^2)^{3/2} (\delta_2 - i\sigma \delta_3) ((\phi_2 + \phi_3 \cos(2\hat{\omega})) \cos \beta - i \sin(2\hat{\omega}) \phi_3)), \quad (15)$$

where $\hat{\omega} = \omega + \gamma$. These expressions contain a number of dimensionless quantities we go on to define below.

1. Dimensionless quantities appearing in the expressions for the torque components

The three dimensionless quantities δ_1 , δ_2 and δ_3 are determined by a strength of energy dissipation in the primary and its angular frequency of rotation, Ω_r . Their formal definitions are as follows

$$\delta_1 = 2\tilde{\Gamma}\tilde{\Omega}, \quad \delta_2 = \lambda\sigma\delta_1, \quad \text{and} \quad \delta_3 = -2\beta_*\lambda\sigma\tilde{\Omega}^2, \quad (16)$$

where $\tilde{\Gamma}$, defined as $\tilde{\Gamma} = \Gamma/\omega_{eq}$, is a characteristic rate of energy dissipation and ω_{eq} is a characteristic dynamical time defined in IP that is associated with tidal disturbance of the primary.

We expect that $\omega_{eq} \sim \Omega_* \equiv \sqrt{GM_*/R_*^3}$, where M_* and R_* are the primary mass and radius, respectively. On the other hand it is expected that $\Gamma \ll \Omega_*$. $\tilde{\Omega} = n_0/\omega_{eq}$, where n_0 is the orbital angular frequency³. The dimensionless quantity $\lambda = 2\beta_*/(2\beta_* + 1)$, where β_* is a dimensionless parameter associated with the Coriolis force (see IP), it is expected to

³ In table 2 of IP $\hat{\Omega}$ erroneously appears instead of $\tilde{\Omega}$ which should replace it.

be smaller than, but order of unity. Similarly the dimensionless quantity $\sigma = \Omega_r/(\lambda n_o)$, is potentially of order unity.

Note too that both δ_1 and δ_2 are proportional to the energy dissipation rate, while δ_3 is determined by rotational effects. Accordingly the terms proportional to δ_3 lead to non-dissipative evolution of the system. The quantities ϕ_1, ϕ_2 , and ϕ_3 are functions of the eccentricity, e , given by

$$\phi_1 = 1 + \frac{15}{2}e^2 + \frac{45}{8}e^4 + \frac{5}{16}e^6, \quad (17)$$

$$\phi_2 = 1 + 3e^2 + \frac{3}{8}e^4 \quad \text{and} \quad (18)$$

$$\phi_3 = \frac{3}{2}e^2 + \frac{1}{4}e^4. \quad (19)$$

2. General torque scaling

All of the torque components are proportional to a characteristic torque magnitude, T_* , given by

$$T_* = \frac{6\pi}{5} \left(\frac{GM_p Q_{eq}}{a^3(1-e^2)^3 \omega_{eq}} \right)^2 = \frac{3k_2 q^2}{1+q} \left(\frac{R_*^5}{a^5} \right) \frac{M_* n_o^2 a^2}{(1-e^2)^6}, \quad (20)$$

where G is gravitational constant, M_* and M_p are respectively the masses of the primary star and compact component, $q = M_p/M_*$ is the mass ratio, a is the orbital semi-major axis and Q_{eq} is the overlap integral (see IP for its formal definition). The quantity Q_{eq} has the dimensions of, $\sqrt{M_*} R_*$, and is expected to be smaller than one when expressed in this unit. The overlap integral can be related to the apsidal motion constant, k_2 , as can be seen by inspection of the second equality in (20).

B. The rate of change of the orbital energy

The rate of change of the orbital energy is given by IP in the form

$$\frac{dE_{orb}}{dt} = \dot{E}_* \left(\delta_2 \phi_1 \cos \beta - \frac{\delta_1}{(1-e^2)^{3/2}} \phi_4 \right), \quad (21)$$

$$\text{where} \quad \dot{E}_* = 2n_o T_* \quad \text{and} \quad (22)$$

$$\phi_4 = 1 + \frac{31}{2}e^2 + \frac{255}{8}e^4 + \frac{185}{16}e^6 + \frac{25}{64}e^8. \quad (23)$$

C. The evolution equations for the Euler angles and the angular momentum vectors

The rate of change of the absolute values of orbital and spin angular momentum vectors and the angles determining their orientation with respect to the primary centred coordinate system follow from equations (11) and (12) after substitution of the components of the torque obtained from equations (14) and (15). Accordingly we obtain

$$\frac{di}{dt} = -(1 - e^2)^{3/2} \sin \beta \frac{T_*}{L} (\sigma \delta_3 \phi_3 \cos \beta \sin 2\hat{\omega} + \delta_2 (\phi_2 - \phi_3 \cos 2\hat{\omega})), \quad (24)$$

$$\frac{d\delta}{dt} = -\frac{T_*}{S} \sin \beta (2\delta_1 \phi_1 - (1 - e^2)^{3/2} (\delta_2 \cos \beta (\phi_2 + \phi_3 \cos 2\hat{\omega}) + \sigma \delta_3 \phi_3 \sin 2\hat{\omega})), \quad (25)$$

$$\begin{aligned} \frac{d\alpha_r}{dt} = -\frac{d\bar{\alpha}}{dt} = -\frac{JT_*}{SL} & \left((\delta_3 \phi_1 - (1 - e^2)^{3/2} (\sigma \delta_3 \cos \beta (\phi_2 + \phi_3 \cos 2\hat{\omega}) + \delta_2 \phi_3 \sin 2\hat{\omega})) \right. \\ & \left. + \frac{1}{3} (1 - e^2)^{9/2} \frac{1+q}{q} \lambda^2 \sigma^2 \cos \beta \right) \end{aligned} \quad (26)$$

and we note that the rate of change of the angle of inclination between the spin and orbital angular momenta is

$$\frac{d\beta}{dt} = \frac{di}{dt} + \frac{d\delta}{dt}. \quad (27)$$

The rate of change of the magnitudes of the orbital and spin angular momenta are respectively given by

$$\frac{dL}{dt} = -2T_* (\delta_1 \phi_1 - (1 - e^2)^{3/2} \delta_2 \phi_2 \cos \beta) - (1 - e^2)^{3/2} T_* \sigma \delta_3 \phi_3 \sin^2 \beta \sin 2\hat{\omega}, \quad (28)$$

and

$$\frac{dS}{dt} = T^z, \quad (29)$$

where T^z is given by equation (14).

Note that in addition to the expression for the torque component T^y in equation (26) given by equation(15) (see equation(11)) we have added a contribution T_{SF}^y arising from the effect of stellar flattening due to rotation. This produces the last term in equation (26) which has the factor $(1 + q)/q$, where $q = M_p/M_*$ is the mass ratio. While our 'standard' torque component T^y is proportional to the stellar rotational frequency Ω_r , T_{SF}^y is proportional to the square of Ω_r , hence the factor σ^2 in this term.

We recall that J is the conserved total angular momentum of the system, while i and δ are, respectively, the angles of inclination between this and the orbital and spin angular momenta. In addition the quantities ϕ_i are given by equations (17)-(19) and (23) with T_* and \dot{E}^* being given by equations (20) and (22).

D. Evolution of the semi-major axis and eccentricity

For Keplerian orbits the relationship between the rate of change of the semi-major axis and the rate of change of orbital energy is given by

$$\frac{da}{dt} = \frac{2a^2}{GM_p M_*} \frac{dE_{orb}}{dt} = \frac{2a^2}{GM_p M_*} \dot{E}_* \left(\delta_2 \phi_1 \cos \beta - \frac{\delta_1 \phi_4}{(1-e^2)^{3/2}} \right), \quad (30)$$

where we have used the expression for dE_{orb}/dt given by equation (21). The rate of change of the orbital eccentricity is given in terms of the rates of change of orbital angular momentum and energy by

$$\frac{de}{dt} = \frac{a(1-e^2)}{GM_p M_* e} \left(\frac{dE_{orb}}{dt} - \frac{dL}{dt} \frac{\sqrt{G(M_p + M_*)}}{a^{3/2} \sqrt{1-e^2}} \right) \quad (31)$$

Substituting (21) and (28) in (31) we obtain

$$\begin{aligned} \dot{e} = & -\frac{3ae(1-e^2)^{-1/2} \dot{E}_*}{GM_p M_*} (3\delta_1 \phi_5 - \frac{11}{6} \delta_2 \phi_6 (1-e^2)^{3/2} \cos \beta) - \\ & \frac{3ae(1+e^2/6)(1-e^2)^2 \dot{E}_*}{4 GM_p M_*} \sigma \delta_3 \sin^2 \beta \sin 2\hat{\omega}, \end{aligned} \quad (32)$$

where we use equation (19) to obtain ϕ_3 and

$$\phi_5 = (\phi_4 - (1-e^2)\phi_1)/(9e^2) = 1 + \frac{15}{4}e^2 + \frac{15}{8}e^4 + \frac{5}{64}e^6 \quad (33)$$

and

$$\phi_6 = \frac{2(\phi_1 - (1-e^2)\phi_2)}{11e^2} = 1 + \frac{3}{2}e^2 + \frac{1}{8}e^4. \quad (34)$$

V. THE CONSERVATIVE ORBITAL EVOLUTION RESULTING FROM ROTATIONAL EFFECTS

As mentioned above in Section IV A 1 our evolution equations contain two types of terms - those proportional to δ_1 and δ_2 , and, accordingly, to the energy dissipation rate characterised by, Γ , and those proportional to δ_3 , which are associated with conservative rotational effects.

The former group of terms may be shown to lead to an equivalent description to that discussed in EKH after an appropriate mapping between the two formalisms is made (see IP). However, note that, our formalism has the advantage that it allows one to relate directly the quantities governing the system evolution driven by the energy dissipation rate to well defined properties of the primary star. The latter group of terms leads to qualitatively new effects. We review them below.

Considering the terms in the tidal response that are $\propto \delta_3$ we neglect dissipative effects in the primary. formally setting $\delta_1 = \delta_2 = 0$. The tidal interaction then conserves orbital energy and consists of an interaction between the spin and orbital angular momenta, characteristically leading to changes in their mutual inclination, accompanied by their precession around the total angular momentum vector. It is important to stress that this approximation may be adequate for sufficiently short time intervals, since the dimensionless parameters $\tilde{\Gamma}^{-1}$ and $\tilde{\Gamma}_p^{-1}$ which determine the timescale of evolution due to the presence of non conservative effects are expected to be relatively quite large.

In addition to the conservation of the orbital energy, it follows from the fact that the Z component of the torque $T^z = 0$ when $\delta_{1,2} = 0$ that the magnitude of the rotational angular momentum, S , is an integral of the motion. Also, from the second equation in the set of (11) together with equation (13) it follows that there is additional integral of motion

$$I = \frac{L^2}{2S} + L \cos \beta, \quad (35)$$

which is valid for any form of T^x .⁴

Since eccentricity e depends only on L when the orbital energy, and, accordingly, semi-major axis a are fixed, from equations (13) and (15) it follows that the evolution equation for $\dot{\beta}$ is a function of β , e and $\hat{\omega}$ when a and S are fixed. From equations (13) and (15), where we set we set $\delta_2 = 0$ and $\delta_3 = -2\beta_* \lambda \sigma \tilde{\Omega}^2$ and remember that $\tilde{\Omega} = n_0/\omega_{eq}$ it is seen that it has the form

$$\dot{\beta} = \left(\frac{1}{S} + \frac{\cos \beta}{L} \right) T_* \frac{3(2\beta_* + 1)e^2(1 - e^2)^{3/2}}{2\tilde{\omega}_{eq}^2} \left(1 + \frac{e^2}{6} \right) \left(\frac{\Omega_r}{\Omega_*} \right)^2 \sin \beta \sin 2\hat{\omega}, \quad (36)$$

where $\Omega_* = \sqrt{GM_*/R_*^3}$ is a typical 'stellar' frequency and $\tilde{\omega}_{eq} = \omega_{eq}/\Omega_* \sim 1$.

⁴ Note a misprint in IP, where there should be $-$ instead of $+$ in (35).

The evolution equation for e follows from (32)

$$\dot{e} = -\frac{3(2\beta_* + 1)ae(1 + e^2/6)(1 - e^2)^2 \dot{E}_*}{4 \tilde{\omega}_{eq}^2 GM_p M_*} \left(\frac{\Omega_r}{\Omega_*} \right)^2 \sin^2 \beta \sin 2\hat{\omega}, \quad (37)$$

where we remember that $\lambda = 2\beta_*/(2\beta_* + 1)$. Note that the same equation can be also obtained by differentiating (35) in time and substituting (36) into the result.

In [10] it was assumed that the rate of change of $\hat{\omega}$ is determined by classical tidal distortion and is given by

$$\frac{d\hat{\omega}}{dt} = \frac{d\varpi}{dt} \equiv \frac{d\varpi_T}{dt} = 15k_2 n_0 \frac{M_p R_*^5}{M_* (a(1 - e^2))^5} \phi_6, \quad (38)$$

(see e.g. [20]), where ϕ_6 is given by eq. (34). and (28) still applies. In [11] and in this paper we consider all potentially important effects causing apsidal precession in an isolated binary star with one point-like component:

$$\frac{d\varpi}{dt} = \dot{\varpi}_T + \dot{\varpi}_E + \dot{\varpi}_R + \dot{\varpi}_{NI}, \quad (39)$$

where $d\varpi_T/dt$ is given by (38),

$$\frac{d\varpi_E}{dt} = \frac{3GM_*(1 + q)}{c^2 a(1 - e^2)} n_0, \quad (40)$$

is the standard expression for the Einstein relativistic apsidal precession, c is speed of light, and

$$\dot{\varpi}_R = -\frac{(3 \cos^2 \beta - 1)}{2} \Omega_Q, \quad \dot{\varpi}_{NI} = -\frac{J}{S} \cos \beta \cos i \Omega_Q \equiv -\frac{(L + S \cos \beta)}{S} \cos \beta \Omega_Q, \quad (41)$$

with

$$\Omega_Q = -\frac{k_2(1 + q)}{(1 - e^2)^2} \left(\frac{R_*}{a} \right)^5 \left(\frac{\Omega_r}{n_0} \right)^2 n_0, \quad (42)$$

being determined by rotational flattening of the primary star. Derivation of the expressions (41) are given by [11] making use of a general expression provided by [2]. Physically, $\dot{\varpi}_R$ is determined by corrections to Keplerian gravitational potential of the primary star due to its rotational flattening, while $\dot{\varpi}_{NI}$ is due to evolution of the orbital frame, which leads to non-inertial effects causing additional apsidal precession.

Remembering that a and Ω_r are constant in case of non-dissipative evolution, using the standard expression for the orbital angular momentum L and expressing the stellar angular momentum in terms of Ω_r as $S = I\Omega_r$, where I is stellar moment of inertial, it is easy to see that equations (36), (37) and (39) form a complete set.

VI. SOME EXAMPLES OF NUMERICAL SOLUTIONS OF THE DYNAMICAL EVOLUTION EQUATIONS

We solve equations (36), (37) and (39) by a standard Runge-Kutta procedure of fourth order. We use the 'slow' time variable $\tau = t/t_*$, where

$$t_* = \frac{\tilde{a}^{13/2} \Omega_*^{-1}}{15k_2 q \sqrt{(1+q)}}, \quad (43)$$

where we have introduced a dimensionless semi-major axis $\tilde{a} = a/R_*$. From equation (38) it is seen that t_* is a characteristic timescale of tidal apsidal precession at small values of eccentricity.

We assume that the dimensionless quantities $\tilde{I} = I/(0.1M_*R_*^2)$, $\alpha_E = (M_*/M_\odot)(k_2/10^{-2})^{-1}(R_*/R_\odot)^{-1}$ and $\gamma_* = (2\beta_* + 1)/(2\omega_*^2)$ are all equal to unity. We consider three different values of mass ratio $q = M_p/M_*$, $q = 10^{-3}$, $q = 1$ and $q = 10^3$. In the first two cases the dimensionless semi-major axis is set to be $\tilde{a} = 5$, while in the large mass ratio case it is set to be $\tilde{a} = 50$. Calculations are performed for a range of initial inclination angles, β_0 . The dimensionless rotation frequencies adopted are $\tilde{\Omega}_r = \Omega_r/n_0 = 0.1, 1$ and 3 . The initial eccentricities were $e_0 = 0.5$ and 0.7 while the initial value of the apsidal angle $\varpi_0 = \pi/4$ for all runs.

All runs start at $\tau = 0$ and end when $\tau = \tau_{end}$, where $\tau_{end} = \frac{6\pi}{t_* \dot{\varpi}_{max}}$ and $\dot{\varpi}_{max} = \sqrt{\dot{\varpi}_T^2 + \dot{\varpi}_E^2 + \dot{\varpi}_R^2 + \dot{\varpi}_{NI}^2}$. Since we are going to present only results of a rather limited number of runs that extend over a limited time span, and the parameter space of the problem is quite large it is clear that the results presented here should be considered as being only preliminary and indicative.

When choosing values of \tilde{a} and $\tilde{\Omega}_r$ it is important to remember that those values are constrained by physical conditions, (see also [11]). At first, it is clear that the orbit periastron, $r_p = (1 - e)a$, should be larger than the stellar radius R_* . Secondly, periastron cannot be smaller than than tidal disruption radius $r_T = (M_1/M_*)^{1/3}R_* = q^{1/3}R_*$. In general, we have

$$\tilde{a} > \tilde{a}_{min} = \frac{\max(1, q^{1/3})}{(1 - e)}. \quad (44)$$

Also, the rotational frequency Ω_r should be smaller by some factor than Ω_* for our theory to be valid. As in [11] we assume that $\Omega_r < 0.5\Omega_*$ (see e.g. [8] for a discussion), thus obtaining

$$\tilde{\Omega}_r < \tilde{\Omega}_{max} = \frac{\tilde{a}^{3/2}}{2\sqrt{1+q}}. \quad (45)$$

In [11] it is shown that when $\tilde{\Omega}_r$ is large and β_0 is chosen in such a way when cancellation between different terms in (39) does not occur, a typical variation of β , $\Delta\beta$, is expected to be

$$\Delta\beta \sim 9q \frac{e^2(1+e^2/6)}{(1-e^2)^3} \tilde{a}^{-3} \sin \beta_0. \quad (46)$$

In what follows we compare (46) with the results of our numerical runs. It was also shown in [10] that cancellation between terms on the right hand side of (39) is expected close to 'critical' values of β_0 , β_{crit} , defined by the condition that $\cos^2(\beta_{crit}) = 1/5$ and on some 'critical' curves $\tilde{a} = a_{crit}(\tilde{\Omega}_r, \beta_0)$ defined by the condition that the right hand side of (39) is zero on the curve. From the condition $\cos^2(\beta_{crit}) = 1/5$ we have $\beta_{crit,\pm} \approx 1.107, 2.03$ corresponding to prograde and retrograde rotation, respectively. Note that critical curves exist only when $\beta > \beta_{crit,+}$. When a solution crosses the critical curve in the course of its evolution its behaviour changes drastically. In this case we expect large variations of β and oscillatory (librating) behaviour of the apsidal angle. We demonstrate explicit examples of such solutions below.

In general, it is expected that the evolution of our system is periodic, with a period smaller than τ_{end} . During this evolution the angle β changes periodically, while $\hat{\varpi}$ could either secularly increase its value (circulate) or have an oscillatory behaviour (librate). In order to characterise the behaviour of our dynamical system over the run time we introduce $\Delta\varpi = \hat{\varpi} - \varpi_0$ and $\Delta\beta = \beta - \beta_0$. Since it is expected that $\Delta\beta$ may change its sign over the evolution we evaluate its maximum value over the time interval $(0, \tau_{end})$, and plot it as a function of the system parameters and initial values of the dynamical variables. We also plot the final value of $\Delta\varpi$.

A. The case $q = 10^{-3}$

We begin by considering the case $q = 10^{-3}$. In Figs. 2 and 3 we respectively show the maximum value of $\Delta\beta = \beta - \beta_0$, $(\Delta\beta)_{max}$, over the time of computation and the final value of $\Delta\varpi = \varpi - \varpi_0$ as functions of β_0 . One can see that $(\Delta\beta)_{max}$ is rather small in this case. This is especially the situation for the small relative rotational frequency $\tilde{\Omega}_r = 0.1$, where $(\Delta\beta)_{max} \sim 10^{-6} - 10^{-5}$ depending on the value of the initial eccentricity. Curves corresponding to $\tilde{\Omega}_r = 1$ and $\tilde{\Omega}_r = 3$ give similar results with larger values of, $(\Delta\beta)_{max}$, corresponding to larger initial eccentricity. The maximum value of the expression (46) during

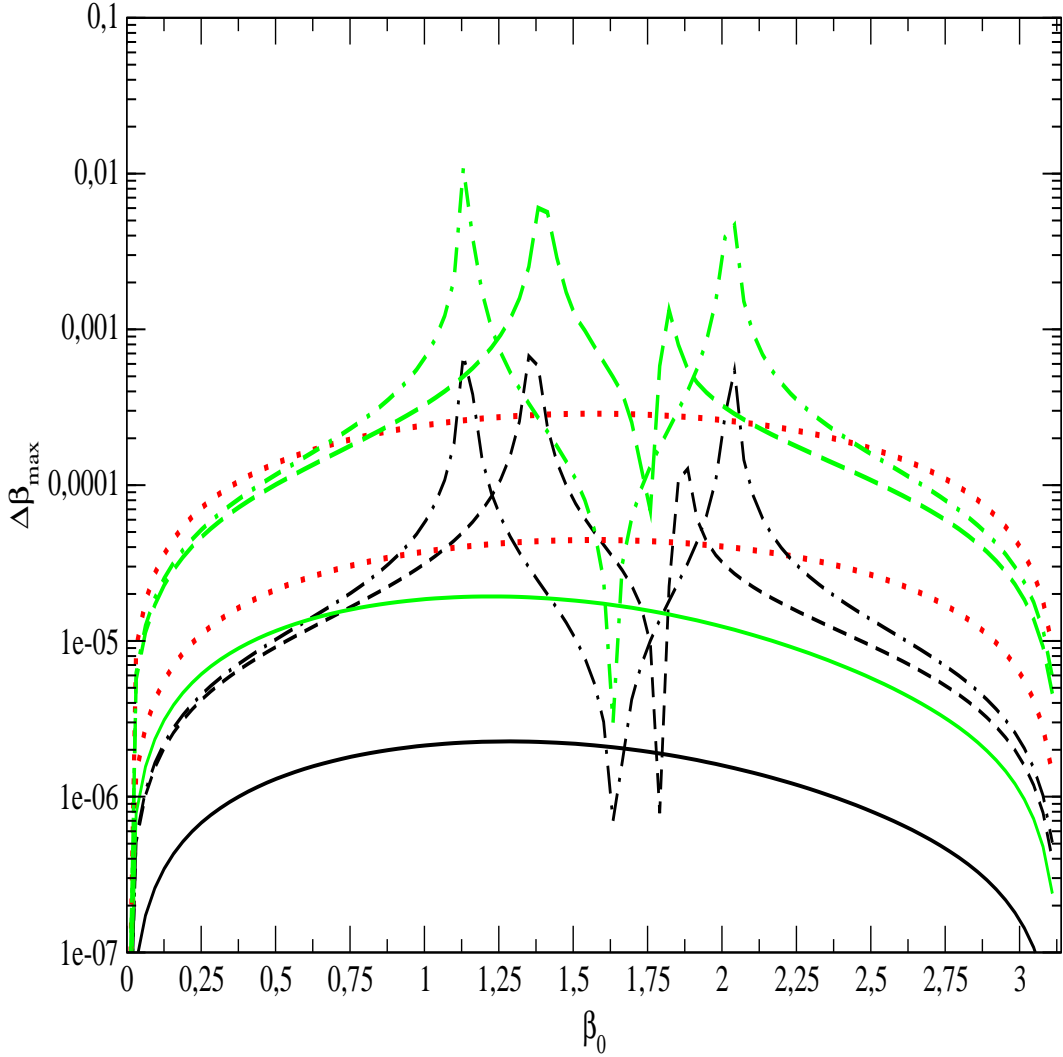


Figure 2: The maximum value of $\Delta\beta$, $\Delta\beta_{max}$, during a run is shown as a function of the initial inclination angle β_0 for $q = 10^{-3}$. Solid, dashed, and dot dashed curves are for $\tilde{\Omega}_r = 0.1, 1$ and 3 , respectively. Dotted curves represent the maximum value of the expression (46). Curves of the same type with larger (smaller) values of their arguments for a given β_0 are calculated for $e_0 = 0.7$ (0.5).

a run provides a reasonable order of magnitude estimate of $(\Delta\beta)_{max}$ when $\beta_0 < \beta_{crit,+}$ and $\beta_0 > \beta_{crit,-}$. In the intermediate range there are two maxima in the neighbourhood of $\beta_{crit,\pm}$ and a minimum in the neighbourhood of $\beta_0 = \pi/2$. From Fig. 3 one can see that the final apsidal angle increases when $\beta_0 < \beta_{crit,+}$ and $\beta_0 > \beta_{crit,-}$, decreases in the intermediate range

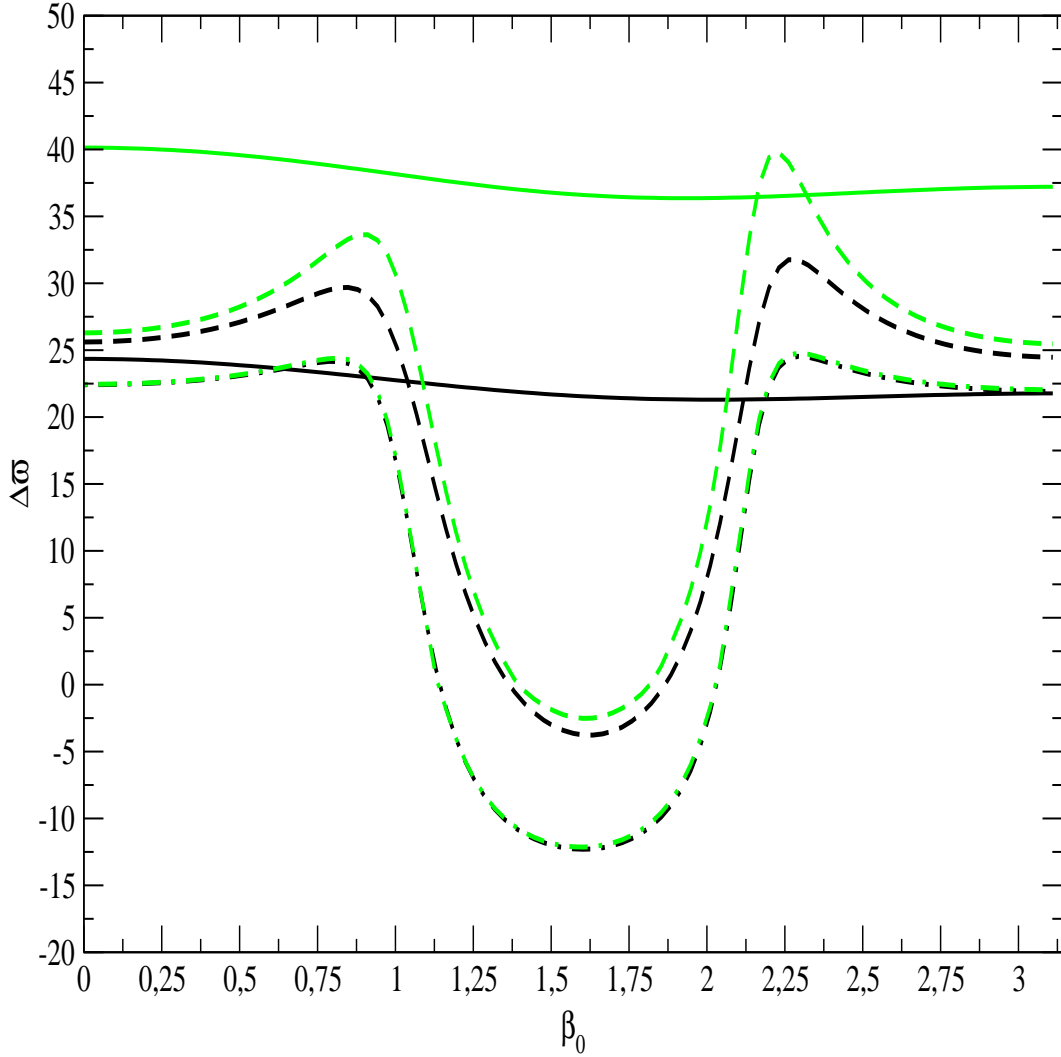


Figure 3: As for Fig. 2, but the final values of the difference $\Delta\varpi$ are shown.

and in close to zero when $\beta_0 \sim \beta_{crit,\pm}$. The latter observation accounts for the existence of two peaks in the distribution of $(\Delta\beta)_{max}$ observed in Fig. 2.

In Fig. 4 and 5 we show the dependence of $\Delta\beta$ and $\Delta\varpi$ on time respectively. The results are for $\beta_0 = 0.5$ and 1, and with $e_0 = 0.5$ and 0.7 in each case. One can see that $\Delta\beta$ is periodic with small amplitude in all cases, the largest amplitude of variation of $\Delta\beta$ is seen in the case of $\beta_0 = 1$ and $e = 0.7$ consistently with the results shown in the previous Figures. From Fig. 5 it is seen that the dependence of $\hat{\varpi}$ on time is practically linear in all cases. The rate of change of $\hat{\varpi}$ increases with increase of initial eccentricity and decreases with

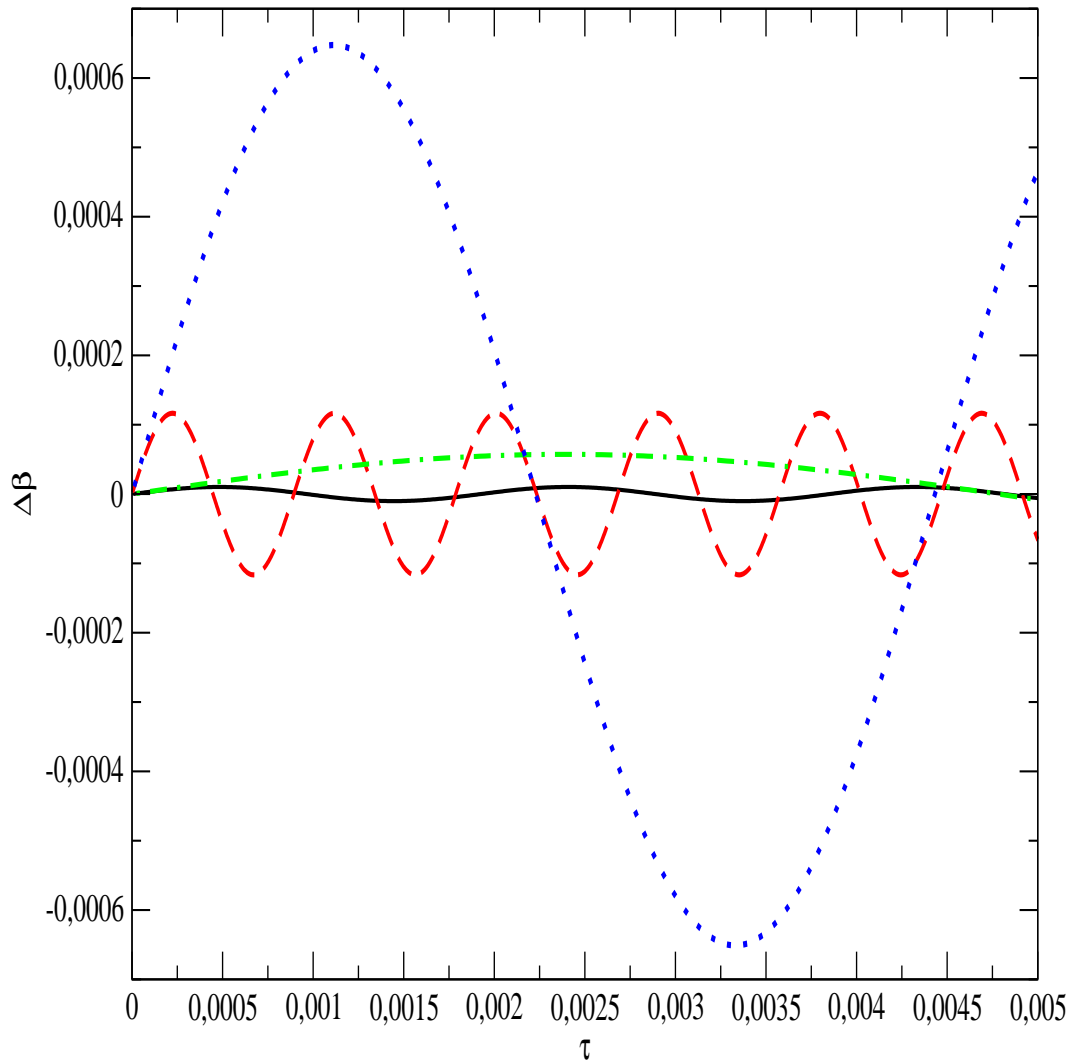


Figure 4: This illustrates the time evolution of the difference $\Delta\beta = \beta - \beta_0$. All curves have $\tilde{\Omega}_r = 3$. Solid and dashed curves have $\beta_0 = 0.5$ with $e_0 = 0.5, 0.7$, respectively. Dot dashed and dotted curves have $\beta_0 = 1$ with $e_0 = 0.5$ and 0.7 , respectively. Note that the latter value of β_0 is close to $\beta_{crit,+}$.

increase of β_0 as expected.

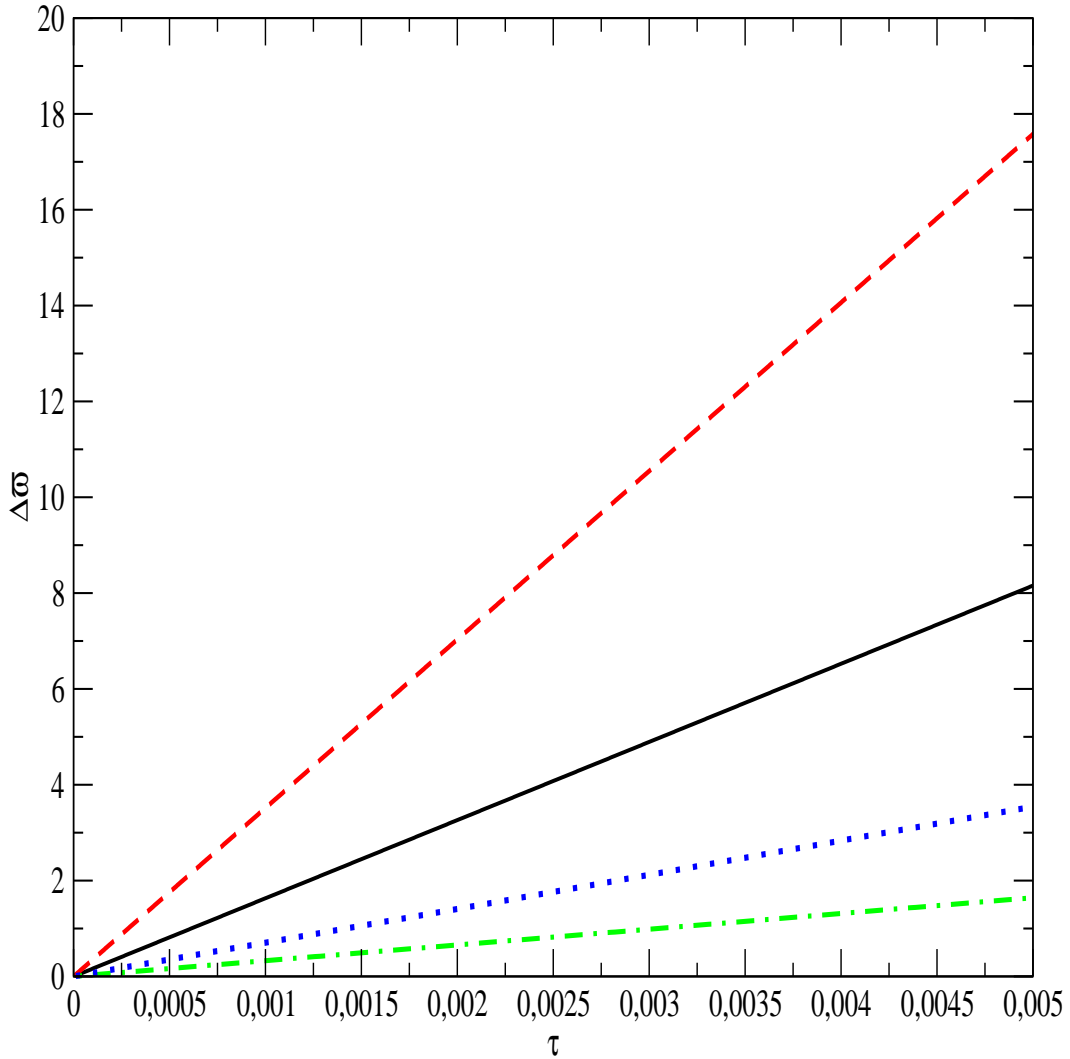


Figure 5: The same as Fig. 4, but the relative values of the apsidal angle $\Delta\varpi = \hat{\varpi} - \varpi_0$ are shown.

B. The case $q = 1$

In Figs. 6 and 7 we respectively show the maximum value of $\Delta\beta = \beta - \beta_0$ and the final value of $\Delta\varpi = \varpi - \varpi_0$ as functions of β_0 calculated for $q = 1$. One can see that the situation is quite different from the previous case. Although the curves corresponding to $\tilde{\Omega}_1 = 0.1$ indicate modest variation of β on the order of $\Delta\beta \sim 10^{-2}$, when $\tilde{\Omega}_1 = 1$ or 3 variations can be significantly larger when $\beta_0 > \beta_{crit,+}$. Only when $\beta_0 < \beta_{crit,+}$ does the maximum value of the expression (46) give a correct order of magnitude estimate for the values of e_0 considered.

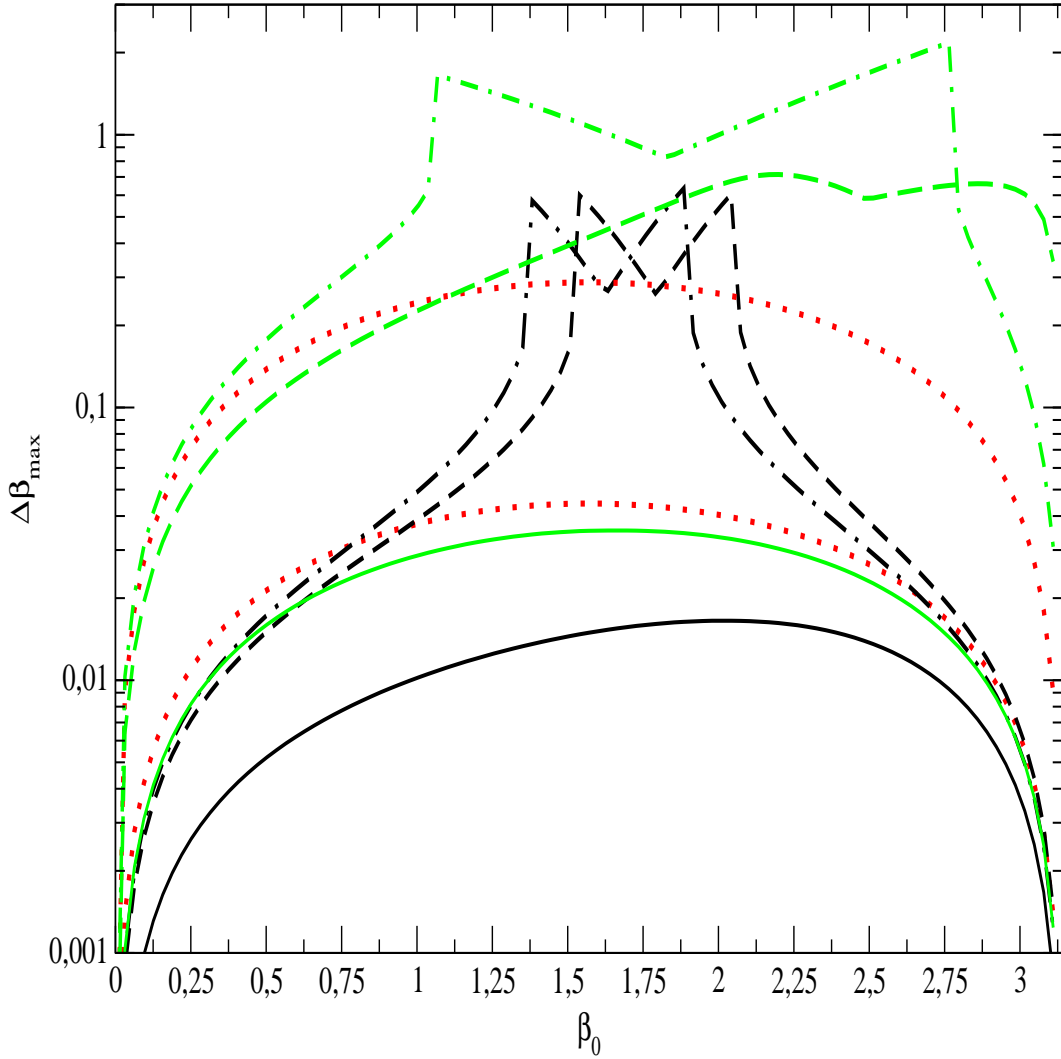


Figure 6: Same as Fig. 2, but for $q = 1$.

When $e_0 = 0.5$ it also gives a correct estimate when $\beta > \beta_{crit,-}$. Otherwise variations are much larger. This effect is interpreted as the evolution of the solutions in the regime where a critical curve is crossed. Let us recall that this is possible only when at some particular moment of time $\beta > \beta_{crit,+}$. When this regime is realised we expect final values of $\Delta\varpi$ to be limited and to remain close to zero in relative terms, since it is accompanied by libration of the apsidal angle. This is seen in Fig. 7, where we have $\Delta\varpi$ close to zero for a range of β_0 in the interval $(\beta_{crit,+}, \beta_{crit,-})$ when $e_0 = 0.5$ and $\tilde{\Omega}_r = 1$, or 3. When $e_0 = 0.7$ we find $\Delta\varpi$ close to zero when $\tilde{\Omega}_r = 3$ and $\beta_{crit,+} < \beta < \sim 2.75$. The case $e_0 = 0.7$, $\tilde{\Omega}_r = 1$ has the usual

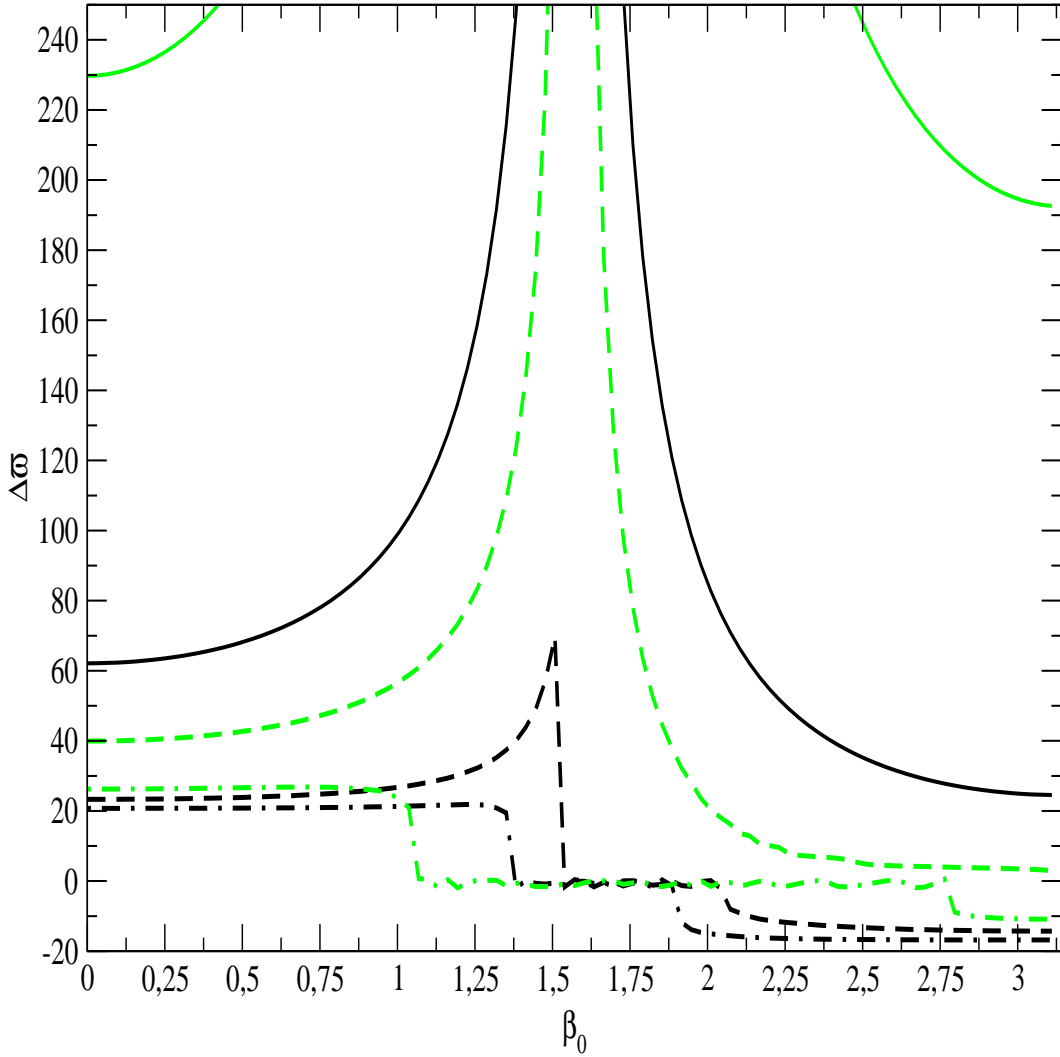


Figure 7: Same as Fig. 3, but for $q = 1$.

circulating regime of evolution of $\hat{\omega}$, but the evolution rate is tending asymptotically to zero when $\beta_0 > \sim 2$. This explains the large values of $(\Delta\beta)_{max}$ in this region of the parameters space.

We further illustrate the case $q = 1$ in Figs 8 and 9, where the evolution of β and $\Delta\varpi$ are shown for $\beta_0 = 0.5$ (solid and dashed curves with $e = 0.5$ and 0.7 , respectively) and $\beta_0 = 2$ (dot dashed and dotted curves with $e = 0.5$ and 0.7 , respectively). In all cases $\tilde{\Omega}_r = 3$. From the discussion above it follows that we expect evolution with librating apsidal angle when $\beta_0 = 2$ and $e = 0.7$. As seen from Fig. 9 this conclusion is confirmed and Fig. 8 shows that

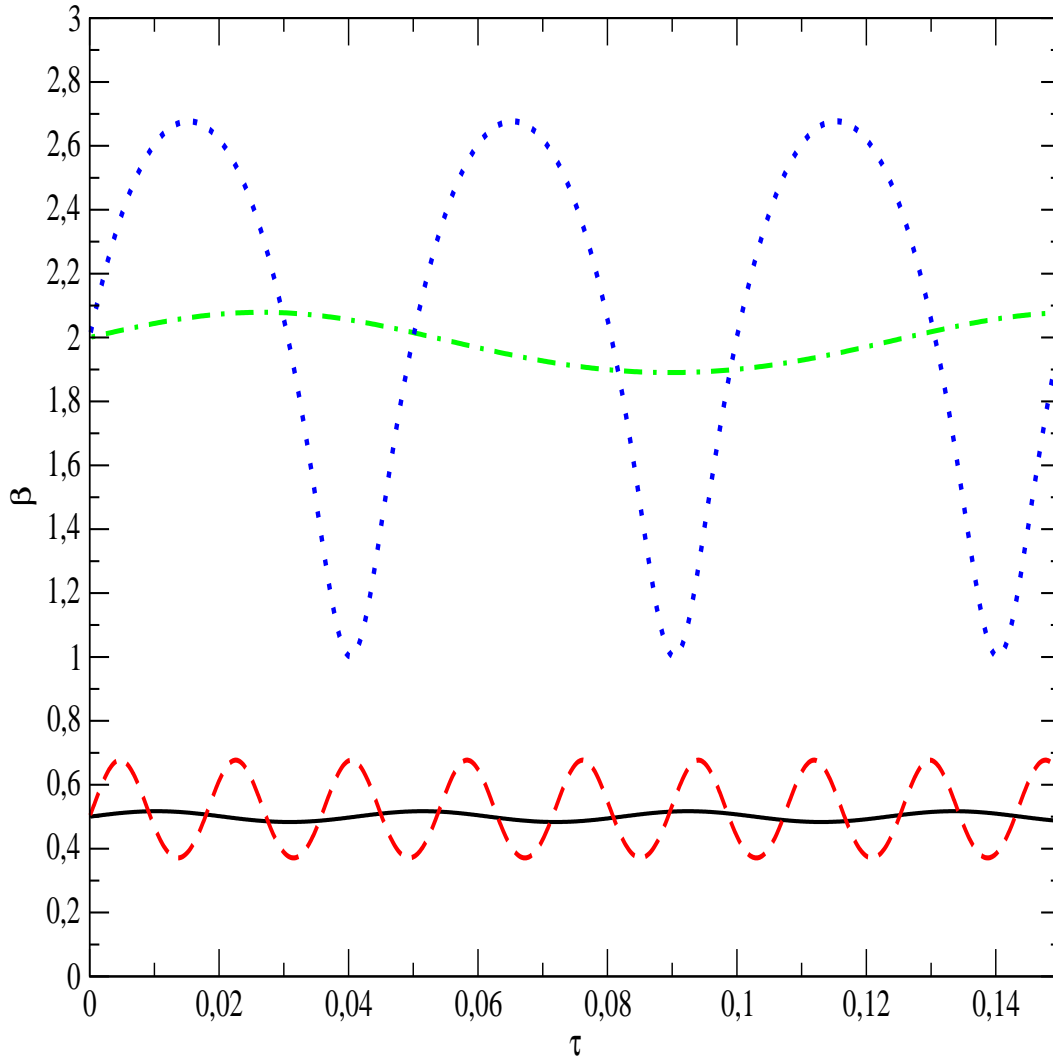


Figure 8: As in Fig. 4, but now we show the time dependence of the inclination angle β for $q = 1$ with $\beta_0 = 0.5$ (solid and dashed curves) and $\beta_0 = 2$ (dot dashed and dotted curves). As for Fig. 4 the larger amplitude variations are for the larger value of e_0 .

in this case variations of β are especially large. Since this angle crosses $\pi/2$ in the course of evolution the system changes its state from prograde to retrograde rotation and vice verse. For an extensive analytic discussion of this regime see [11].

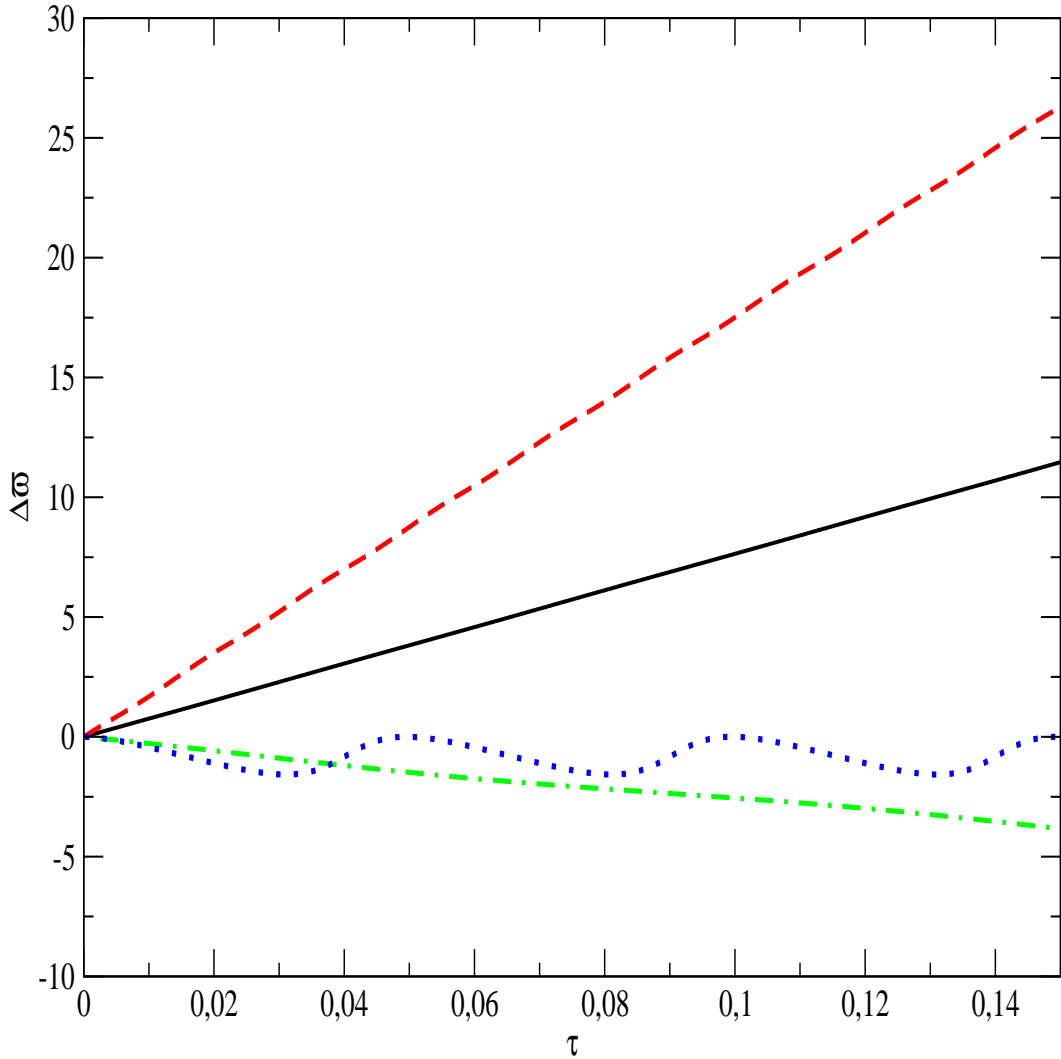


Figure 9: As for Fig. 8, but $\Delta\varpi$ is shown.

C. The case $q = 10^3$

The general behaviour of $(\Delta\beta)_{max}$ and $\Delta\varpi$ in the case $q = 10^3$ is shown in Figs. 10 and 11. Note that unlike the previous cases now \tilde{a} is ten times large, $\tilde{a} = 50$. Since in this case it is assumed that non-dissipative tides are active in a planet of Jupiter size, this choice of \tilde{a} corresponds to approximately the same physical value of semi-major axis as the other cases. In this case especially large variations of β are seen when $1.25 \sim \beta_0 \sim 2$ with $e_0 = 0.5$ and when $0.75 \sim \beta_0 \sim 2.5$ with $e_0 = 0.7$, see Fig. 10. From Fig. 11 it is seen that

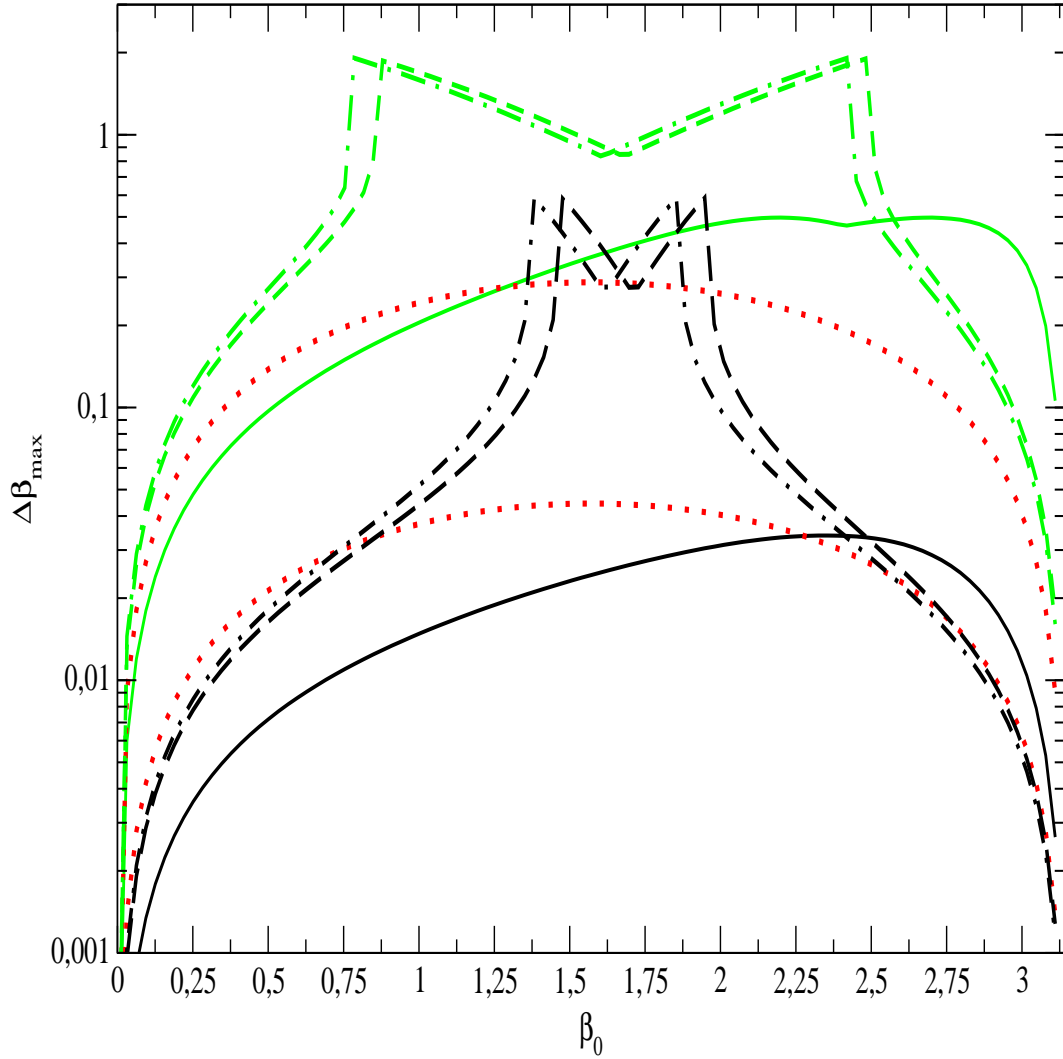


Figure 10: As for Figs. 2 and 6, but $q = 10^3$ and $\tilde{a} = 50$.

indeed in these ranges of β_0 $\Delta\varpi$ is close to zero, and, therefore, the regime of apsidal angle libration is realised.

Figs 12 and 13 show the time dependence of β and $\Delta\varpi$ for $\beta_0 = 0.5$ (solid and dashed curves have $e_0 = 0.5$ and 0.7 , respectively) and $\beta_0 = 0.8$ (dot dashed and dotted curves have $e_0 = 0.5$ and 0.7 , respectively). As in the previous case the regime of apsidal angle libration is expected when $\beta_0 = 0.8$ and $e_0 = 0.7$. Fig. 13 confirms this prediction, while from Fig. 12 we see that variations of β are quite large in this case and the system changes its rotation from prograde to retrograde, very much as in the case $q = 1$.

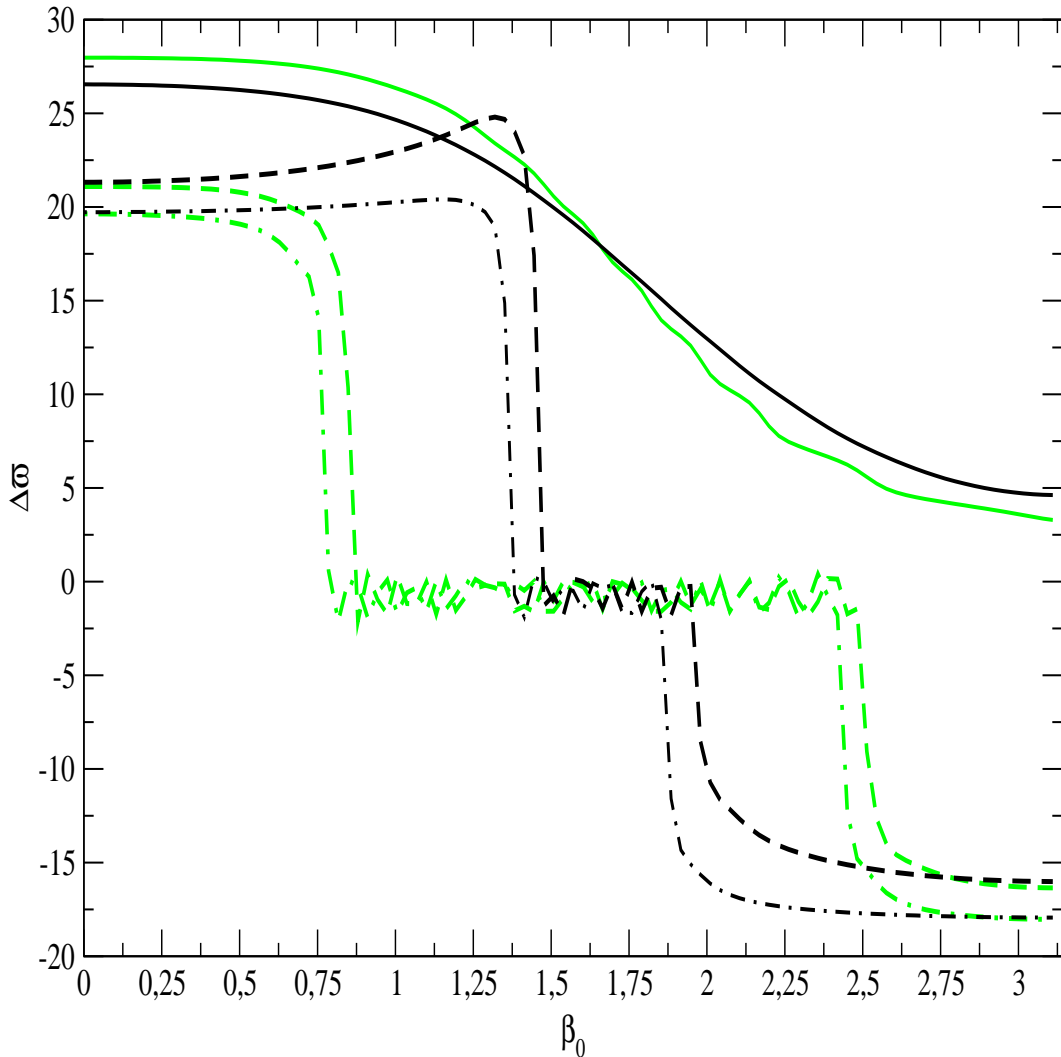


Figure 11: As for Figs. 3 and 7, but $q = 10^3$ and $\tilde{a} = 50$.

VII. DISCUSSION AND CONCLUSIONS

In this paper we reviewed and extended the main results of our paper [10]. There a self-consistent approach to the evolution of the orbital parameters of an eccentric binary with misaligned orbital and spin angular momenta due to quasi-stationary tides was proposed. We described and reviewed both qualitatively and quantitatively the new non-dissipative effects obtained within the framework of our approach, giving the full evolution equations governing them in Section IV C . These effects result from the rotation of the primary. They

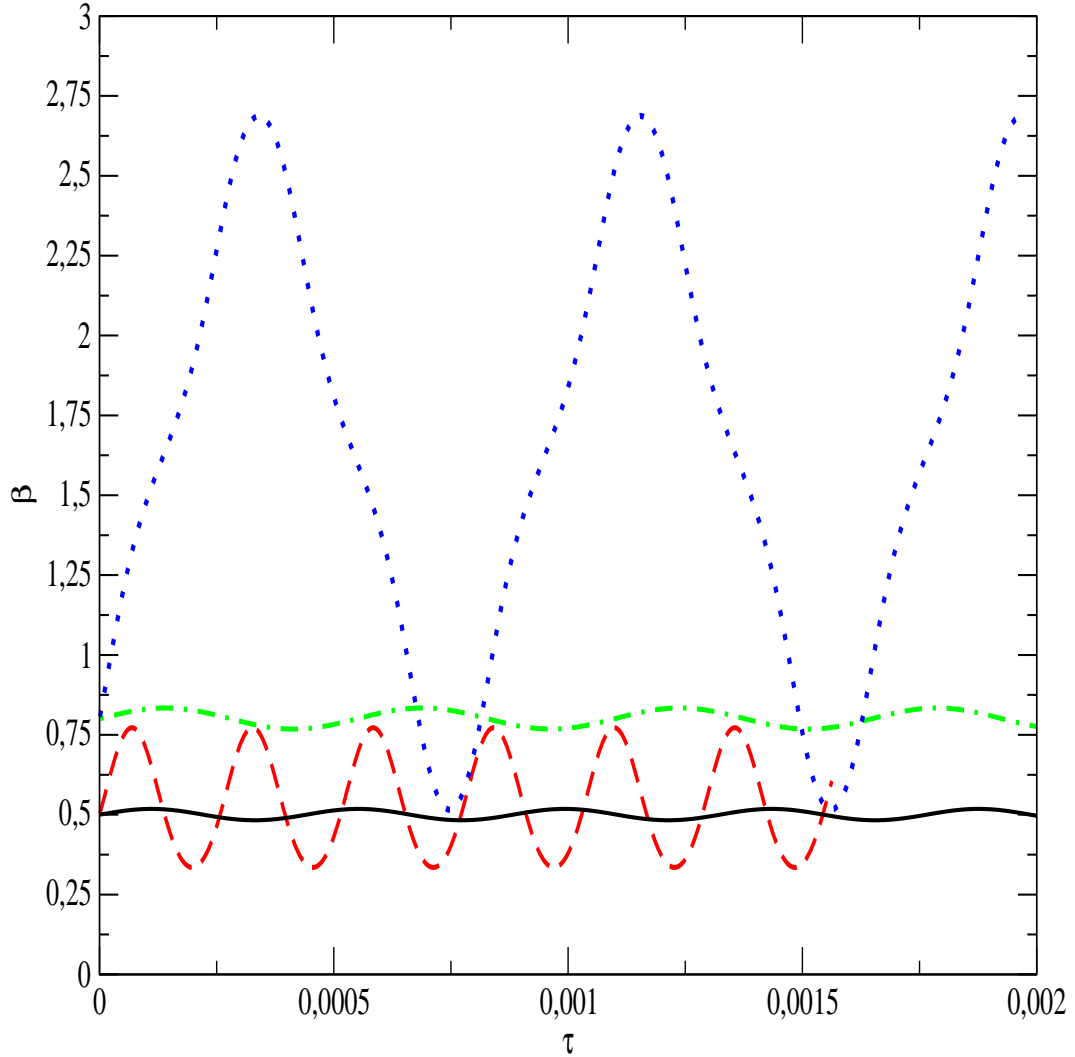


Figure 12: As for Fig. 8, but for $q = 10^3$ with $\beta_0 = 0.5$ (solid and dashed curves) and $\beta_0 = 0.8$ (dot dashed and dotted curves).

cause an evolution of the angle of inclination between the orbital and spin angular momenta, β , on a relatively short time scale provided that the source of apsidal precession is specified.

Unlike the analysis made in [10] we took into account all potentially important sources of apsidal precession for an isolated binary with only one tidally active component. These are Einstein precession, the apsidal precession rate caused by the tidal bulge, and that arising from rotational distortion, see equation (39). Since the apsidal precession rate due to stellar rotation depends on the inclination angle, β , in general the dynamical system describing

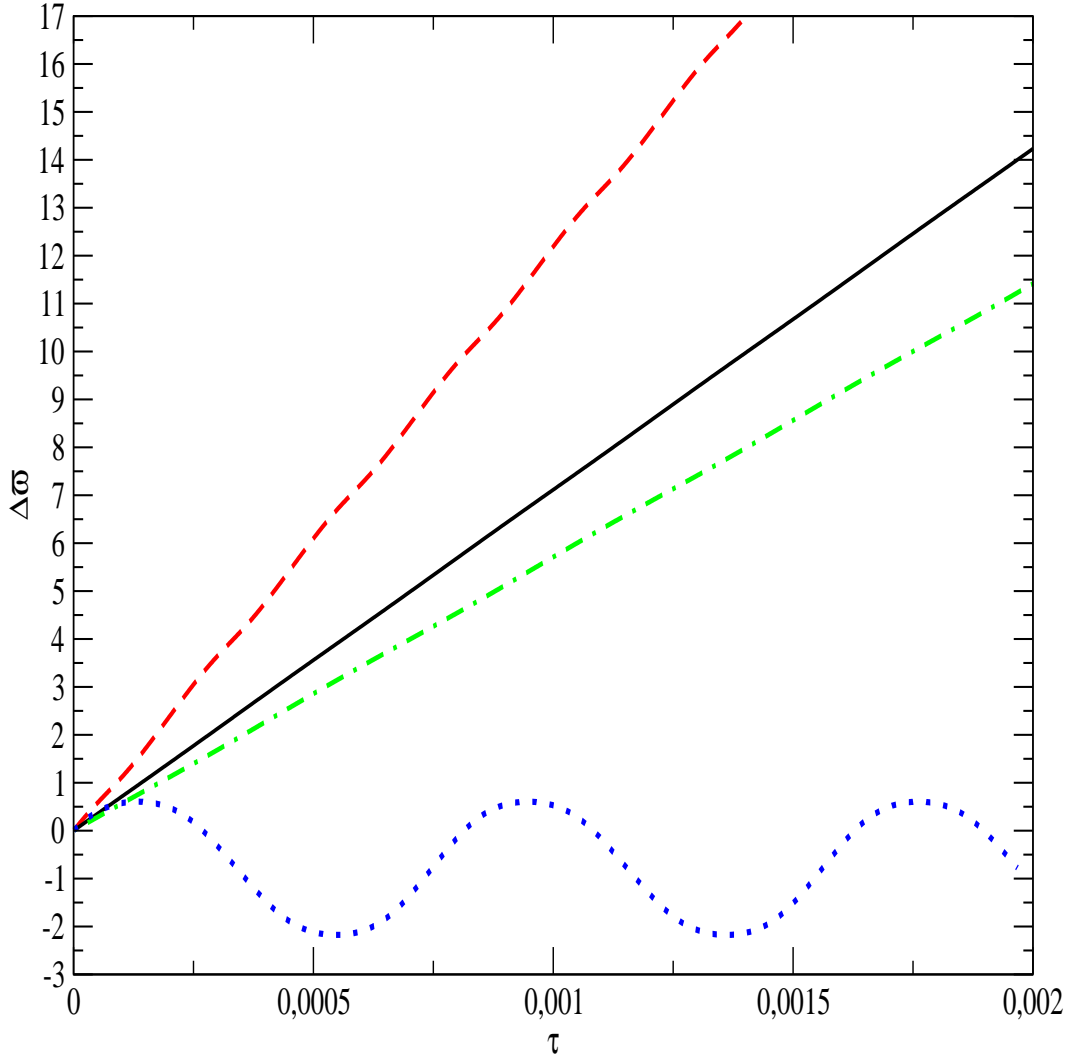


Figure 13: As for Fig. 12, but $\Delta\varpi$ is shown.

the non-dissipative tidal evolution effectively has two degrees of freedom. The presence of non-linear interaction between two angles can lead to qualitatively new effects for certain values of the parameters of the system.

We illustrate these effects by solving the corresponding dynamical equations numerically for an indicative exploratory set of input parameters over a limited time span.. We find that when mass ratio q is small variations of β are expected to be small, and the apsidal angle changes monotonically with time. However, when the mass ratio is order of unity or larger and both stellar rotation and eccentricity are significant periodic variations of β can

be order of unity, and the system can change the direction of its rotation from prograde to retrograde over some relatively short period of time. In the same situation the apsidal angle changes periodically with time. As explained in an accompanying paper [11], where we provide an extensive analytic analysis of the dynamical system, these new effects are related to the possibility of the existence of 'critical curves' - the curves in the parameter space of the system, where the total apsidal precession rate $\dot{\varpi}$ is zero. When the system crosses such a curve during its evolution the apsidal angle librates, while a typical change of β is much larger than that obtained from naive estimates. Observational implications of these results will be reported elsewhere.

There is a simple physical explanation for these new non-dissipative effects. Namely, in the absence of rotational effects (and, of course, while neglecting dissipation) the tidal bulge is aligned with the direction to perturbing body. When the rotation axis is misaligned with respect to orbital angular momentum, the presence of rotational effects, arising from e.g. Coriolis forces, produce torques which lead to the evolution of the angle of inclination between the orbital and spin angular momenta. These do not occur in the aligned case. This resembles in part the well known Lidov-Kozai effect, but, in our case there is no need for the presence of a third body to break the symmetry of gravitational field.

It is important to stress that we have neglected a contribution of toroidal displacements potentially excited by perturbation of the star due to tides. Although it may be small effect due to the relatively small magnitude of the appropriate overlap integrals, this contribution should be separately analysed. A convenient framework for such an analysis would be the self-adjoint approach to the problem of tidal excitation of normal modes of any kind in a rigidly rotating star put forward in [16] and [7].

Finally, let us estimate typical values of $\Delta\beta$ and corresponding evolution times for two potentially interesting systems. We consider systems containing a neutron star with its stellar companion, having a rotation axis significantly misaligned with the orbital angular momentum, such that the inclination angle $\beta_0 \sim 1$. In all cases we assume, for definiteness, that stellar rotation frequency is equal to the orbital angular frequency, and accordingly $\tilde{\Omega}_r = 1$. The evolution time scale of $\Delta\beta$, t_{ev} , is here defined as $t_{ev} = \pi |(d\varpi/dt)^{-1}|$, where $d\varpi/dt$ is given by eq. (39) and it is also assumed that a single term on r.h.s of (39) dominates. To estimate characteristic values of $\dot{\varpi}_R$ and $\dot{\varpi}_{NR}$ we set $3 \cos^2 \beta - 1$ and $\cos \beta$ to be unity in the corresponding expressions, see eq. (41).

At first we consider a system with parameters similar to the parameters of the famous low mass X-ray binary Sco X-1. At the present time its eccentricity e is smaller than $\sim 10^{-2}$, see e.g. [13] and references therein. However, it is reasonable to assume that it has been significantly larger in the past, due to a possible kick during the supernova explosion leading to the formation of the neutron star. The same kick could be responsible for the spin misalignment. To take into account the system's evolution we use initial masses of the donor star, its radius, mass of the neutron star and the orbital period from Table 1 of [6], their model 4, which is realistic according to these authors. Namely, we use $M_* = 0.7M_\odot$, $R_* = 0.53R_\odot$, $M_p = 1.41M_\odot$ and $P_{orb} = 10h$. The values adopted for k_2 and \tilde{I} in this Section are 0.01 and 0.1 respectively.

We consider two values of eccentricity, $e = 0.2$ and $e = 0.5$, and find that in both cases $d\varpi/dt$ is dominated by the non-inertial term, $\ddot{\varpi}_{NI}$ and use, accordingly, eq. (46) to estimate $\Delta\beta$. We obtain $\Delta\beta \approx 4.5 \cdot 10^{-3}$ and $t_{ev} \approx 0.49yr$ for $e = 0.2$, and $\Delta\beta \approx 6.1 \cdot 10^{-2}$ and $t_{ev} \approx 0.34yr$ for $e = 0.5$. It is clear that t_{ev} is much smaller than any characteristic time scale of secular orbital evolution driven by tidal effects. Note that other terms in (39) are smaller than the leading one by at least one order of magnitude for such a system. In this case the presence of the critical curves leading to larger values of $\Delta\beta$ is not expected unless β is extremely close to $\pi/2$.

Next we consider the system GX-301-2, which consists of a hypergiant companion and an X-ray pulsar. We use $M = 43M_\odot$, $R_* = 68R_\odot$, $M_p = 1.85M_\odot$ and $P_{orb} = 45d$ as well as $e = 0.5$, see e.g. [14], [12] and [4]. We see again that $d\varpi/dt$ is dominated by non-inertial term, but, in this case the next to leading term, $\ddot{\varpi}_T$, is just a factor of two smaller, thus there is a possibility of being near a critical curve. Nonetheless, we use (39), (41) and (46) to estimate t_{ev} and $\Delta\beta$ noting that for some plausible system parameters and significant inclination, β , $\Delta\beta$ obtained from (46) could be significantly underestimated. We obtain $t_{ev} \approx 150yr$ and $\Delta\beta \approx 1.1 \cdot 10^{-2}$. It is worth stressing again that t_{ev} is likely to be much smaller than any potential time scale of secular orbital evolution. We note that the hypergiant star in this system exhibits a significant mass loss due to stellar wind, with corresponding mass loss rate $\dot{M}_W \sim 10^{-5}M_\odot/yr$, see e.g. [12]. This is expected to cause orbital evolution on time scale $\sim M_*/\dot{M}_W \sim 10^5 - 10^6yr$. This is two-three orders of magnitude larger than t_{ev} .

Acknowledgments

PBI was supported in part by the grant 075-15-2020-780 'Theoretical and experimental studies of the formation and evolution of extrasolar planetary systems and characteristics of exoplanets' of the Ministry of Science and Higher Education of the Russian Federation. We are grateful to A. J. Barker, K. A. Postnov, N. I. Shakura and the referee for useful comments.

-
- [1] Barker, A. J., Ogilvie, G. I., 2009, MNRAS, 395, 2268
 - [2] Barker, B. M., O'Connell, R. F., 1975, Phys. Rev. D, 12, 329
 - [3] Chernov, S. V., Ivanov, P. B., Papaloizou, J. C. B., 2017, MNRAS, 470, 2054
 - [4] Doroshenko, V., Santangelo, A., Suleimanov, V., Kreykenbohm I., Staubert, R., Ferrigno, C., Klochkov, D., 2010, A&A, 515, A10
 - [5] Eggleton, P. P., Kiseleva, L. G., Hut, P., 1998, ApJ, 499, 853
 - [6] Fedorova A. V., Tutukov, A. V., 2022, Astronomy Reports, 2022, 66, 925
 - [7] Ivanov, P. B., Papaloizou, J. C. B., 2007, MNRAS, 376, 682
 - [8] Ivanov, P. B., Papaloizou, J. C. B., 2007, A&A, 476, 121
 - [9] Ivanov, P. B., Papaloizou, J. C. B., 2011, Celestial Mechanics and Dynamical Astronomy, 111, 51
 - [10] Ivanov, P. B., Papaloizou, J. C. B., 2021, MNRAS, 500, 3335 (IP)
 - [11] Ivanov, P. B., Papaloizou, J. C. B., MNRAS, submitted
 - [12] Kaper, L., van der Meer, A., Najarro, F., 2006 A&A, 457, 595
 - [13] T. L. Killestein, M. Mould, D. Steeghs, J. Casares, D. K. Galloway, J. T. Whelan, 2023, MNRAS, 520, 5317
 - [14] Koh, A. T., Bildsten, L. B., Chakrabarty, D., Nelson, R. W., Prince, T. A., Vaughan, B. A., Finger, M. H., Wilson, R. B., Rubin, B. C., 1997 ApJ, 479, 933
 - [15] Ogilvie, G. I., 2014, ARA&A , 52, 171
 - [16] Papaloizou, J. C. B., Ivanov, P. B., 2005, MNRAS, 364, L66
 - [17] Philippov, A. A., Rafikov, R. R., 2013, ApJ, 768, 112
 - [18] Ragozzine, D., Wolf, A. S., 2009, ApJ, 698, 1778

- [19] Shakura, N. I., 1985, *Soviet Astronomy Letters*, 11, 224
- [20] Sterne, T. E., 1939, *MNRAS*, 99, 451

